

QSCOUT's Qubit-Boson Gate Set

Edward C Tortorici, Ethan C McGarrigle, Brian K McFarland, and Christopher G Yale

April 27, 2026

1 Introduction

The Quantum Scientific Computing Open User Testbed (QSCOUT) [1] has developed a qubit-boson gate set for hybrid continuous-discrete variable (CV-DV) quantum computing. This document outlines how to utilize these gates on QSCOUT using Just Another Assembly Language, JaqalTM [2].

QSCOUT is a trapped-ion quantum processor that utilizes a single, linear chain of Yb-171 ions as a qubit register with all-to-all connectivity. The qubit states used are

$$\begin{aligned} |^2S_{1/2}, F = 0, m_F = 0\rangle &= |0\rangle_{\text{qubit}} \\ |^2S_{1/2}, F = 1, m_F = 0\rangle &= |1\rangle_{\text{qubit}} \end{aligned} \tag{1}$$

with a transition energy of about 12.6 GHz. To avoid confusion, here we use spin to denote the qubit states and integers to denote motional states in the Fock basis. In particular, the qubit states $|0\rangle$ and $|1\rangle$ will be referred to as:

$$\begin{aligned} |0\rangle_{\text{qubit}} &\rightarrow |\downarrow\rangle \\ |1\rangle_{\text{qubit}} &\rightarrow |\uparrow\rangle. \end{aligned} \tag{2}$$

QSCOUT addresses the qubit by driving a Raman transition using two tones ω_1 and ω_2 , such that $\omega_1 - \omega_2 = \omega_c$, where ω_c is the carrier transition frequency for the qubit.

The eigenmodes of the ion chain's collective motion (called motional modes or phonon modes) are utilized as quantum harmonic oscillators (qumodes). To access the motional modes, the Raman transition is driven with two counter-propagating beams. On one side, there is a large beam that globally addresses the ion chain, and on the other side, there are tightly focused beams that individually address each ion [1]. Generally, up to two tones with independent control over amplitude, phase, and frequency modulation can be applied to each beam, and in special cases, four tones can be applied to a single beam. QSCOUT supports pulse-level control in Jaqal via the JaqalPaw interface [3].

A register of N ions will have N flavors of collective motion (see fig. 1), each of which will manifest 3 modes (one for each principal axis) for a total of $3N$ modes. The gate lasers point orthogonal to the axial direction of the ion chain, limiting access to only the $2N$ radial modes. Collective motion encompasses the entire chain, but the coupling strengths of each ion to each mode are not uniform, and some ions have very weak to zero coupling to some modes.

Each flavor of radial mode can be indexed from 0 to $N - 1$, as seen in fig. 1. In Jaqal, this index is referred to as `<mode>`. The trap confinement is elliptical (see fig. 2), such that one set of these N radial modes is higher energy than the other. We refer to these as the upper and lower manifolds and are called out in Jaqal with `<manifold>`, where 0 corresponds to the upper and 1 to the lower manifold. Each qumode then has a unique energy that can be denoted with a frequency $\omega_{f,m}$, where f is the manifold index, and m is the mode index. The ellipticity of the confinement is selected such that $\omega_{0,i} > \omega_{1,j}$ for all i and j , in other words all modes of the upper manifold are higher energy than any mode in the lower manifold. An example of the motional sideband spectrum and how they are identified is shown in fig. 3.

Motional states live in an infinite-dimensional Hilbert space, but for practical purposes, it is often necessary to work in a truncated basis. For example, when working in the Fock basis of phonon-occupation number states $\{|n\rangle, n \geq 0\}$, it becomes increasingly difficult to distinguish Fock states as n increases, and truncating around $|n = 10\rangle$ is recommended given current readout limitations.

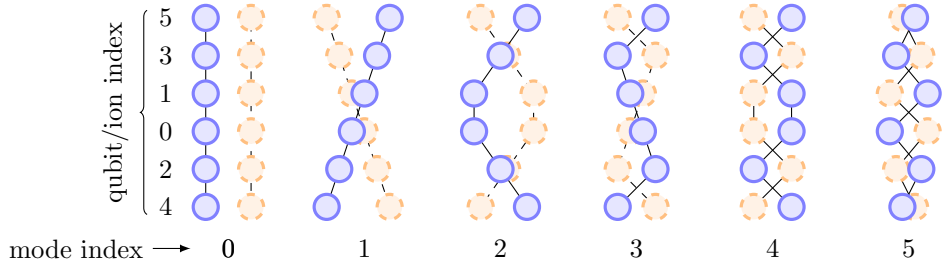


Figure 1: The flavors of radial modes for 6 ions labeled by mode index. Mode 0, the highest energy mode within a manifold, is the center of mass (COM) mode, and mode 1 is the tilt mode. We refer to mode 2 as the drum mode, and the lowest energy mode ($N - 1$) as the zig-zag mode (The remaining modes do not have strong naming conventions as they become more zig-zag-like in nature as the mode number increases). The qubits/ions are indexed starting from the center ion: they are labeled with increasing qubit number, alternating outward from the center, as seen on the left.

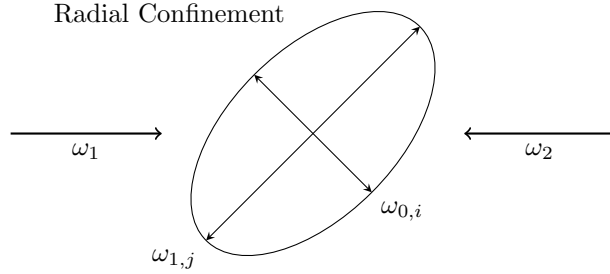


Figure 2: The radial confinement is elliptical, so that the two radial modes of the same mode index have different energies, such that $\omega_{0,i} > \omega_{1,j}$ for all i and all j , where i is the mode index for the upper manifold and j is the mode index for the lower manifold. The two beams driving Raman transitions are orthogonal to the axial direction, so they only project onto the radial modes.

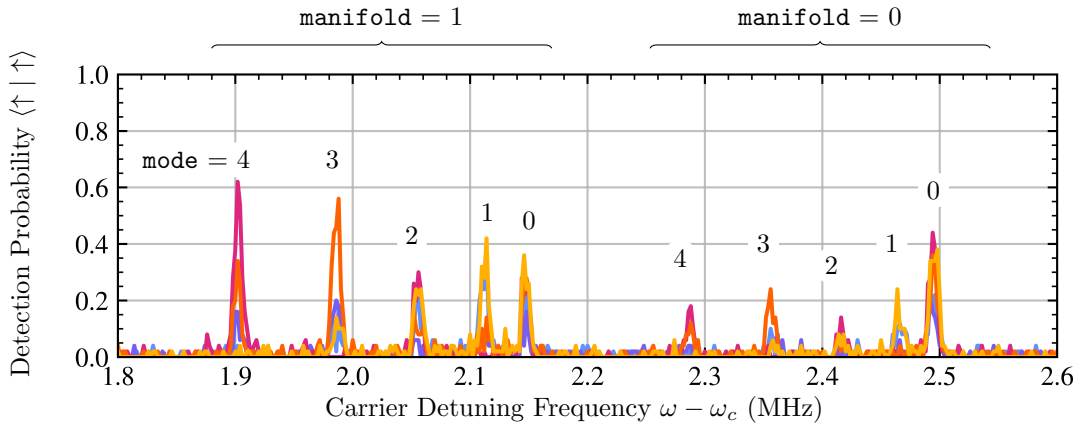


Figure 3: Motional sideband spectrum for 5 ions. The 5 flavors of radial modes each appear twice: one at a lower frequency (**manifold = 1**), and one at a higher frequency (**manifold = 0**). A qumode is then called out by specifying both a manifold and a mode index. The axial frequency manifold does not appear because the lasers do not project onto these modes.

2 The Gates

Gate	Jaqal command
Jaynes-Cummings	JC <qubit> <manifold> <mode> <phase> <angle>
Anti-Jaynes-Cummings	AJC <qubit> <manifold> <mode> <phase> <angle>
Conditional Displacement	xCD <qubit> <manifold> <mode> <Re[beta]> <Im[beta]>
	yCD <qubit> <manifold> <mode> <Re[beta]> <Im[beta]>
	zCD <qubit> <manifold> <mode> <Re[beta]> <Im[beta]>
Conditional Rotation	CR <qubit> <manifold> <mode> <angle>
Conditional Beamsplitter*	BS <qubit> <manifold_1> <mode_1> <manifold_2> <mode_2> <phase> <angle>
Conditional Squeeze*	CSq <qubit> <manifold> <mode> <sq.amp> <sq.phase>

Table 1: The available gates on QSCOUT and their associated Jaqal commands. Qubit indices are labeled 0 to N , starting from the center, as seen in fig. 1. Manifolds and modes are indexed as seen in fig. 3. See sections 2.1 to 2.5 for more details on each gate. *(Gates are in progress/development).

2.1 Jaynes-Cummings

The Jaynes-Cummings gate is a resonant drive on a motional sideband red-detuned from the carrier transition, such that

$$\Delta\omega = \omega_1 - \omega_2 = \omega_c - \omega_{f,m}, \quad (3)$$

where ω_1 and ω_2 are laser tones, with each applied to one of the two of the counter-propagating beams, ω_c is the carrier transition frequency, and $\omega_{f,m}$ is the frequency of the motional mode involved in the interaction.

The Jaynes-Cummings gate can be described by:

$$JC(\theta, \phi) = \exp[-i\theta(e^{i\phi}\sigma_- a^\dagger + e^{-i\phi}\sigma_+ a)]. \quad (4)$$

The gate will either increase or decrease the Fock number conditioned on the spin state:

$$|\downarrow, n+1\rangle \longleftrightarrow |\uparrow, n\rangle, \quad (5)$$

where the qubit state is of the ion that is being addressed by the laser system, and the motional state is of the mode determined by $\omega_{f,m}$. Additionally, the coupling efficiency of the drive increases as $\sqrt{n+1}$ for a given transition between two distinct Fock states, so the effective Rabi rate is

$$\Omega_{\text{eff}} = \sqrt{n+1} \eta \Omega, \quad (6)$$

where Ω is the Rabi rate of the carrier transition, and η is the Lamb-Dicke factor for the mode of interest.

The gate is called with

$$\text{JC } \langle \text{qubit} \rangle \langle \text{manifold} \rangle \langle \text{mode} \rangle \langle \text{phase} \rangle \langle \text{angle} \rangle \quad (7)$$

where the qubit index follows the numbering convention shown in fig. 1, the manifold and mode indices are numbered as shown in fig. 3, the phase (ϕ in eq. (4)) defines the rotation axis on the Bloch sphere (where a phase of 0 is a rotation about the x -axis) in radians, and the angle (θ in eq. (4)) defines how much rotation to apply about the rotation axis in radians.

2.2 Anti-Jaynes-Cummings

The Anti-Jaynes-Cummings gate is a resonant drive on a motional sideband blue-detuned from the carrier transition, such that

$$\omega_1 - \omega_2 = \omega_c + \omega_{f,m}. \quad (8)$$

The gate definition is:

$$AJC(\theta, \phi) = \exp[-i\theta(e^{i\phi}\sigma_+ a^\dagger + e^{-i\phi}\sigma_- a)], \quad (9)$$

and acts similar to the Jaynes-Cummings gate but the condition on the spin state is reversed:

$$|\downarrow, n\rangle \longleftrightarrow |\uparrow, n+1\rangle. \quad (10)$$

The gate is called with

$$\text{AJC } \langle \text{qubit} \rangle \langle \text{manifold} \rangle \langle \text{mode} \rangle \langle \text{phase} \rangle \langle \text{angle} \rangle \quad (11)$$

2.3 Conditional Displacement

The conditional displacement gate performs displacement on the motional state conditioned on the qubit state. This can be done relative to x , y , or z basis:

$$CD(\beta, i) = \mathcal{D}(\beta\sigma_i) = \exp[\sigma_i\beta a^\dagger - \sigma_i^*\beta^* a], \quad (12)$$

where $i \in \{X, Y, Z\}$, and \mathcal{D} is the displacement operator.

The gate is performed by applying a spin-dependent force to an ion. One tone ω_1 is applied to one beam, and two ω_2 and ω_3 are applied to the counter-propagating beam, such that

$$\omega_1 - \omega_2 = \omega_c - \omega_{f,m} \quad (13)$$

$$\omega_1 - \omega_3 = \omega_c + \omega_{f,m}. \quad (14)$$

This is equivalent to running the red and blue sidebands simultaneously. Note that from a practical standpoint, the σ_X and σ_Y gates are the native gates, only differing by programmed phases, whereas the σ_Z version requires additional “wrapper” carrier $\pi/2$ pulses to transform the σ_X version into the σ_Z version.

The gate is called with

$$\langle \text{axis} \rangle \text{CD } \langle \text{qubit} \rangle \langle \text{manifold} \rangle \langle \text{mode} \rangle \langle \text{Re}[\text{beta}] \rangle \langle \text{Im}[\text{beta}] \rangle \quad (15)$$

where the axis is either x , y , or z and defines the Pauli σ_i in eq. (12) and β (**beta**) is the complex-valued displacement.

2.4 Conditional Rotation

The conditional rotation gate accumulates phase on the qubit conditioned on the motional state. The definition of the gate is

$$CR(\theta) = \exp\left[-\frac{i\theta}{2}\sigma_Z a^\dagger a\right]. \quad (16)$$

This gate starts by applying a red sideband with blue detuning δ , such that $\Delta\omega = \omega_c - \omega_{f,m} + \delta$, which causes a Fock-dependent light shift and carrier light shift. This is then echoed with a blue sideband with the same detuning, such that $\Delta\omega = \omega_c + \omega_{f,m} + \delta$, in order to cancel the carrier induced light shift. This results in phase accumulation with an effective Rabi rate of

$$\Omega_{\text{eff}} = \frac{2n\eta^2\Omega^2}{\delta}. \quad (17)$$

We note that this operation currently has a significant decay profile and is best used sparingly, such as reading out the parity of the Fock occupancy.

The gate is called with

$$\text{CR } \langle \text{qubit} \rangle \langle \text{manifold} \rangle \langle \text{mode} \rangle \langle \text{angle} \rangle \quad (18)$$

where the angle, in radians, corresponds to the amount of phase accumulation on the qubit for a Fock state of $n = 1$.

2.5 Gates in Progress

The following gates are currently under development. These gates are based on the theoretical work by Sutherland and Srinivas [4], utilizing two red- and two blue- sideband tones to generate second-order interactions. QSCOUT's control hardware, Octet [1, 5], is currently restricted to two tones per channel. To get more tones, we utilize a feature for cross-talk mitigation, that allows for duplication of neighbor and next-nearest neighbor channels to provide more tones to realize these gates (see section VI-A5 of reference [1]). However, due to the current channel to qubit mapping, these four-tone gates can only be conditioned on specific qubits and require significant calibration overhead.

For both of the following gate protocols, the spin phase of one of the red-blue sideband pairs is set to generate a σ_X interaction, while the the spin phase of the other reb-blue sideband pair generates a σ_Y interaction. The detuned four tones result in a dominant 2-photon σ_Z process that gives either a spin-dependent beamsplitter or spin-dependent squeezing operation. The Hamiltonian for this interaction is described in Sutherland and Srinivas (2021): see eq. (2) in reference [4].

2.5.1 Conditional Beamsplitter

To generate the conditional beamsplitter interaction, the four tones are set up with symmetric detuning, δ , off of the two modes of interest (denoted with $\omega_{f,m}$ and $\omega_{f',m'}$), as follows:

$$\omega_1 - \omega_2 = \omega_c - \omega_{f,m} + \delta \quad (19)$$

$$\omega_1 - \omega_3 = \omega_c + \omega_{f,m} - \delta \quad (20)$$

$$\omega_1 - \omega_4 = \omega_c - \omega_{f',m'} + \delta \quad (21)$$

$$\omega_1 - \omega_5 = \omega_c + \omega_{f',m'} - \delta. \quad (22)$$

which leads to the following operation, which swaps the Fock occupancy of one mode with the occupancy of another mode:

$$BS(\theta, \phi) = \exp \left[-\frac{i\theta}{2} \sigma_Z (a^\dagger b e^{i\phi} + ab^\dagger e^{-i\phi}) \right], \quad (23)$$

where a and a^\dagger are the annihilation and creation operators for the first mode $\omega_{f,m}$, and b and b^\dagger are the annihilation and creation operators of the second mode $\omega_{f',m'}$. This parametrization aligns with Sutherland and Srinivas (2021) [4] when shifting the phase definition $\phi \rightarrow \phi \pm \pi/2$.

The gate will be called with

$$\text{BS } \langle \text{qubit} \rangle \langle \text{manifold}_1 \rangle \langle \text{mode}_1 \rangle \langle \text{manifold}_2 \rangle \langle \text{mode}_2 \rangle \langle \text{phase} \rangle \langle \text{angle} \rangle \quad (24)$$

where the two modes involved in the beamsplitter must be defined, and angle defines the rotation of the gate on the Bloch sphere in radians (where an angle of π corresponds to full swap of population between the modes). The beamsplitter phase ϕ can be set by setting the motional phase on one of the sideband pairs to ϕ while setting the other sideband pairs' motional phase to zero.

2.5.2 Conditional Squeeze

To generate the conditional squeeze operation, the four tones are detuned, δ , above and below the mode of interest with motional sideband frequency ω_m :

$$\omega_1 - \omega_2 = \omega_c - \omega_{f,m} + \delta \quad (25)$$

$$\omega_1 - \omega_3 = \omega_c - \omega_{f,m} - \delta \quad (26)$$

$$\omega_1 - \omega_4 = \omega_c + \omega_{f,m} + \delta \quad (27)$$

$$\omega_1 - \omega_5 = \omega_c + \omega_{f,m} - \delta. \quad (28)$$

which can lead to the following operation, squeezing the motional state:

$$CSq(\zeta) = \exp \left[-\frac{\sigma_Z}{2} (\zeta^* a^2 - \zeta a^{\dagger 2}) \right] \quad (29)$$

where $\zeta = r e^{i\phi}$ is the complex-valued spin-dependent squeezing parameter. The squeezing phase ϕ can be set by setting the motional phase on one of the sideband pairs to ϕ while setting the other sideband pairs' motional phase to zero.

The gate will be called with

$$\text{CSq } \langle \text{qubit} \rangle \langle \text{manifold} \rangle \langle \text{mode} \rangle \langle \text{sq.amp} \rangle \langle \text{sq.phase} \rangle \quad (30)$$

where the amplitude and phase define the complex squeezing amplitude ζ .

3 State Preparation

State Preparation	Jaqal command
Vacuum state	Prepared by default
Fock state	<code>FockStatePrep</code> $\langle \text{qubit} \rangle \langle \text{manifold} \rangle \langle \text{mode} \rangle \langle \text{n_fock} \rangle$
Squeezed vacuum state	<code>RampSqPrep</code> $\langle \text{qubit} \rangle \langle \text{manifold} \rangle \langle \text{mode} \rangle \langle \text{sq_amp} \rangle \langle \text{sq_phase} \rangle$

Table 2: The available state preparation functions on QSCOUT.

3.1 Vacuum State

Sideband cooling is used to prepare a thermal state very near $|0\rangle$. We typically measure an average occupation of about 0.1 quanta after sideband cooling in non-COM modes. This is the default preparation for all quantum circuits and is already contained within the `prepare_all` command required for all `Jaqal` circuits.

3.2 Fock State

To prepare a Fock state, after sideband cooling, alternating *AJC* and *JC* π -pulses are used to continuously flip the spin and increase the Fock state by one. However, the effective Rabi rate increases as the Fock state increases, so each successful pulse is shortened to accommodate this. A so-called prep qubit is typically chosen to perform these operations on, but can be reused for other operations if desired.

Sideband cooling prepares $|\downarrow, 0\rangle$, and each gate flips the spin and increases the Fock number by one, so possible states in the Fock state preparation procedure are either $|\downarrow, 2k\rangle$ (spin-down with even Fock state) or $|\uparrow, 2k+1\rangle$ (spin-up with odd Fock state) with $k \in \mathbb{Z}^+$. During this process, the Anti-Jaynes-Cummings gate is applied to $|\downarrow, 2k\rangle$ to increase the Fock number and flip the spin:

$$AJC\left(\frac{\pi}{\sqrt{n+1}}, 0\right) |\downarrow, n\rangle = |\uparrow, n+1\rangle, \quad (31)$$

while the Jaynes-Cummings gate is applied to odd $|\uparrow, 2k+1\rangle$ to increase the Fock number and flip the spin:

$$JC\left(\frac{\pi}{\sqrt{n+1}}, 0\right) |\uparrow, n\rangle = |\downarrow, n+1\rangle. \quad (32)$$

Preparing an even Fock state applies the following operations:

$$\text{even } n : \quad JC\left(\frac{\pi}{\sqrt{n}}, 0\right) \dots AJC\left(\frac{\pi}{\sqrt{3}}, 0\right) JC\left(\frac{\pi}{\sqrt{2}}, 0\right) AJC(\pi, 0) |\downarrow, 0\rangle = |\downarrow, n\rangle, \quad (33)$$

and since an odd Fock state ends with an Anti-Jaynes-Cummings, a final π -rotation is applied to return the qubit to the $|\downarrow\rangle$:

$$\text{odd } n : \quad R_X(\pi) AJC\left(\frac{\pi}{\sqrt{n}}, 0\right) \dots AJC\left(\frac{\pi}{\sqrt{3}}, 0\right) JC\left(\frac{\pi}{\sqrt{2}}, 0\right) AJC(\pi, 0) |\downarrow, 0\rangle = |\downarrow, n\rangle. \quad (34)$$

3.3 Squeezed Vacuum

Eigenstates of the JC Hamiltonian do not require the four-tone conditional squeeze gate and can be prepared via a method involving fewer tones. First, consider the Hamiltonian with both JC and AJC terms with coupling strengths g_1 and g_2 respectively:

$$H = g_1(\sigma_+ a + \sigma_- a^\dagger) + g_2(e^{i\phi}\sigma_+ a^\dagger + e^{-i\phi}\sigma_- a). \quad (35)$$

This can be recast with a different set of annihilation and creation operators: b, b^\dagger , with

$$\begin{aligned} b &= \cosh(|\zeta|)a + e^{i\phi} \sinh(|\zeta|)a^\dagger \\ &= S(\zeta)aS^\dagger(\zeta), \end{aligned} \quad (36)$$

where

$$S(\zeta) = \exp \left[\frac{1}{2}(\zeta^* a^2 - \zeta a^{\dagger 2}) \right] \quad (37)$$

and ζ is the squeezing parameter with magnitude

$$\zeta = \tanh \left(\frac{g_2}{g_1} \right) e^{i\phi}, \quad (38)$$

thus forming the recast Hamiltonian:

$$H = \sqrt{|g_1^2 - g_2^2|} (\sigma_+ b + \sigma_- b^\dagger). \quad (39)$$

The practical implementation of this Hamiltonian is to start with a red-sideband (JC) pulse on with the blue-sideband (AJC) adiabatically ramping up to the desired ratio g_2/g_1 which sets the squeeze parameter ζ . For more information about this operation on QSCOUT, see reference [6]. The vacuum ground state $|\downarrow, 0\rangle$ being an eigenstate of the JC Hamiltonian can be squeezed in this way.

4 Measurement

There are currently two primary tools for reading out motional state information on QSCOUT, and there is interest in building out more measurement tools through user projects.

4.1 Measure of Fock State Occupation

An arbitrary motional state can be described in the Fock basis

$$|\psi\rangle_{\text{motional}} = \sum_{n=0}^{\infty} c_n |n\rangle, \quad (40)$$

where c_n are complex valued and $|c_n|^2 = p_n$ are Fock occupancies, with

$$1 = \sum_{n=0}^{\infty} p_n. \quad (41)$$

The effective Rabi rate when driving an Anti-Jaynes-Cummings gate is described by eq. (6), and for a state described in the Fock basis, each Fock state will drive according to

$$AJC(t) |\downarrow, n\rangle = \cos \left(\eta\Omega\sqrt{n+1} t \right) |\downarrow, n\rangle + \sin \left(\eta\Omega\sqrt{n+1} t \right) |\uparrow, n+1\rangle, \quad (42)$$

The probability of detecting $|\uparrow\rangle$ after driving the gate for time t will then be

$$P_\uparrow(t) = \langle \downarrow, \psi | AJC^*(t) |\uparrow\rangle \langle \uparrow | AJC(t) |\downarrow, \psi\rangle = \frac{1}{2} \left[1 - e^{-t/T_2} \sum_n p_n \cos \left(\eta\Omega\sqrt{n+1} t \right) \right], \quad (43)$$

where T_2 is the coherence time. By measuring the probability of the $|\uparrow\rangle$ qubit state for variable Anti-Jaynes-Cummings gate time (this requires several shots), a data set of $P_\uparrow(t)$ vs t can be fit for $|a_n|^2$ for n up until some reasonable cutoff. An example dataset to illustrate the method is provided in section 4.1

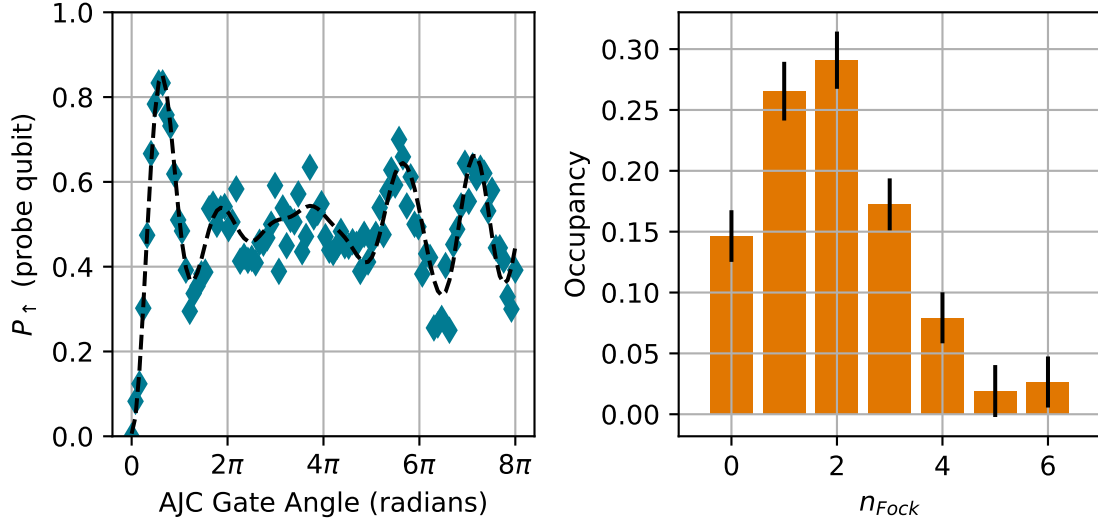


Figure 4: Example Fock State Occupancy Measurement. (left) The resultant beating oscillations from Fock occupation measurement via AJC gate. The oscillations are fit to eq. (43) to extract the Fock occupancies p_n presented on the (right).

4.2 Measure of the Characteristic Function of the Motional Phase Space

Motional tomography can be performed by reading out the characteristic function in motional phase space using the conditional displacement gate on a properly prepared probe qubit, as seen in fig. 5. The expectation value for the concluding Z measurement on the probe qubit is

$$\langle Z \rangle = \cos \theta \Re[\chi(\beta)] + \sin \theta \Im[\chi(\beta)], \quad (44)$$

where θ is the angle applied to the $R_x(\theta)$ gate seen in fig. 5, β is a complex-valued position in the motional phase space, and χ is the characteristic function:

$$\chi(\beta) = \langle \mathcal{D}(\beta) \rangle, \quad (45)$$

where $\mathcal{D}(\beta)$ is the displacement operator. Therefore, when a θ of $\pi/2$ is used, this measurement reads out $\Im[\chi]$ and when no rotation is applied, the measurement reads out $\Re[\chi]$. An example of motional tomography data taken on the QSCOUT, in this way, is shown in fig. 6.

The characteristic function is closely related to the Wigner representation, which is a pseudo probability density of the motional state in phase space:

$$\mathcal{W}(\gamma) = \frac{1}{\pi^2} \int \chi(\beta) e^{\gamma\beta^* - \gamma^*\beta} d^2\beta, \quad (46)$$

where γ , like β is a complex-valued position in phase space. This is a 2D Fourier transform that does an inverse Fourier transform from $\Re[\beta]$ to $\Im[\gamma]$ and a forward Fourier transform from $\Im[\beta]$ to $\Re[\gamma]$.

This measure requires several probes of the motional state at a particular β in order to establish a reasonable estimate of $\langle Z \rangle$. It is possible to build out a full picture of the phase space by probing a grid of β values, but this

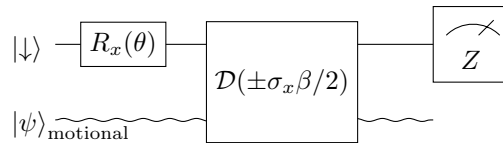


Figure 5: The circuit used to probe the characteristic function $\chi(\beta)$ by way of the conditional displacement gate $\mathcal{D}(\pm\sigma_x\beta/2)$ on a probe qubit.

is a very time consuming endeavor. We suggest, in general, probing as little of the phase space as necessary; for example, a 1D cross section may be all that is needed to obtain the needed information to understand the state.

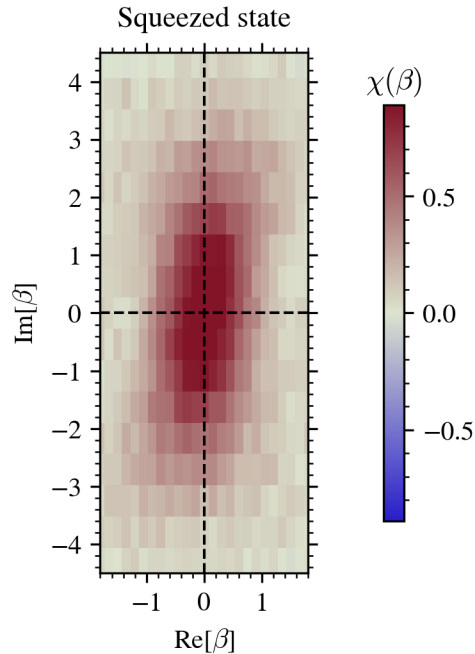


Figure 6: Example motional tomography data of a squeezed vacuum state.

5 Acknowledgments

Sandia National Laboratories is a multimission laboratory managed and operated by National Technology & Engineering Solutions of Sandia, LLC, a wholly owned subsidiary of Honeywell International Inc., for the U.S. Department of Energy’s National Nuclear Security Administration under contract DE-NA0003525.

References

- [1] S. M. Clark, D. Lobser, M. C. Revelle, C. G. Yale, D. Bossert, A. D. Burch, M. N. Chow, C. W. Hogle, M. Ivory, J. Pehr, B. Salzbrener, D. Stick, W. Sweatt, J. M. Wilson, E. Winrow, and P. Maunz. Engineering the Quantum Scientific Computing Open User Testbed. *IEEE Transactions on Quantum Engineering*, 2:1–32, 2021. ISSN 2689-1808. doi: 10.1109/TQE.2021.3096480. URL <https://ieeexplore.ieee.org/document/9483669/>.
- [2] Andrew J. Landahl, Daniel S. Lobser, Benjamin C. A. Morrison, Kenneth M. Rudinger, Antonio E. Russo, Jay W. Van Der Wall, and Peter Maunz. Jaqal, the quantum assembly language for QSCOUT, March 01, 2020 2020. URL <https://arxiv.org/abs/2003.09382>. 14 pages, 0 figures.
- [3] Daniel Lobser, Joshua Goldberg, Andrew J. Landahl, Peter Maunz, Benjamin C. A. Morrison, Kenneth Rudinger, Antonio Russo, Brandon Ruzic, Daniel Stick, Jay Van Der Wall, and Susan M. Clark. JaqalPaw: A guide to defining pulses and waveforms for Jaqal, 2023. URL <https://arxiv.org/abs/2305.02311>.
- [4] R. T. Sutherland and R. Srinivas. Universal hybrid quantum computing in trapped ions. *Phys. Rev. A*, 104: 032609, Sep 2021. doi: 10.1103/PhysRevA.104.032609. URL <https://link.aps.org/doi/10.1103/PhysRevA.104.032609>.

- [5] Daniel S. Lobser, Jay W. Van Der Wall, and Joshua D. Goldberg. Performant coherent control: bridging the gap between high- and low-level operations on hardware. In *2022 IEEE International Conference on Quantum Computing and Engineering (QCE)*, pages 320–330, 2022. doi: 10.1109/QCE53715.2022.00053.
- [6] Sungjoo Lim, Chanyang Im, Christopher G. Yale, Brian K. McFarland, Edward C. Tortorici, Daniel S. Lobser, Melissa C. Revelle, Susan M. Clark, Mahn-Soo Choi, and Junki Kim. Observation of the topological edge state of the generalized resonant Rabi model in a trapped-ion quantum simulator. *in preparation*, 2026.